JOURNAL OF CATALYSIS **179,** 129–137 (1998)
ARTICLE NO. CA982212

Effect of Cationic Promoters on the Kinetics of Ammonia Synthesis Catalyzed by Ruthenium Supported on Zeolite X

Thierry Bécue,* Robert J. Davis,*,[1] and Juan M. Garces†

*Department of Chemical Engineering, University of Virginia, Charlottesville, Virginia 22903; †Dow Chemical Company, Catalysis R&D, 1776 Building, Midland, Michigan 48674

Received March 24, 1998; revised June 25, 1998; accepted June 29, 1998

Zeolite-X-supported ruthenium materials (2 wt% Ru) were synthesized, characterized, and tested as catalysts for ammonia synthesis at 20 bar. The effects of both cation type (K, Cs, Mg, Ba) and loading (exchanged or occluded) on the kinetics of ammonia synthesis were evaluated. Residual protons in the ion exchanged catalysts were detrimental to both zeolite stability and measured turnover frequency. In addition, alkaline-earth-exchanged materials were more active than alkali-exchanged materials, contrary to the ranking of zeolite basicity. Successive impregnations of Ba cations beyond ion exchange capacity of Ru/BaX further promoted the ammonia synthesis reaction by almost an order of magnitude to levels near that of Cs-promoted Ru/MgO, a highly active, nonzeolitic catalyst. Impregnation of occluded K cations onto Ru/KX did not improve catalyst activity, presumably due to the severe loss in micropore volume during reaction. Orders of reaction for the Ru/BaX catalysts were about 1 and −1 for N_2 and H_2, respectively, which is consistent with N_2 adsorption being rate-determining and hydrogen atoms covering a substantial fraction of the metal surface.

Key Words: **ruthenium; ammonia; nitrogen; hydrogen; zeolite X; potassium; cesium; magnesium; barium; kinetics.**

INTRODUCTION

In the early 1970s, Ozaki and co-workers introduced a new catalyst for ammonia synthesis consisting of ruthenium metal supported on carbon and promoted by alkali metal (Ru/AC-M, where AC is activated carbon and M is an alkali metal) (1, 2). At 523 K and 80 kPa, Ru/AC-K exhibited a tenfold increase in the rate of NH_3 synthesis, compared to a conventional promoted iron catalyst under similar conditions (1, 2). Since then, a promoted Ru/carbon catalyst has been developed for use in the Ocelot Ammonia Plant in British Columbia. In addition to lower capital costs, the energy consumption in this plant was reduced by 1 million BTU/ton of ammonia synthesized, compared with iron-based systems (3).

[1] To whom correspondence should be addressed.

Although activated carbon was the support for Ru in the pioneering work of Ozaki *et al.* (1, 2), Ru catalyzes the oxidation and methanation of carbon (4, 5). Therefore, a more stable support is desirable. Zeolites are of particular interest as supports for metals since the maximum size of the intracrystalline particles is limited to the size of the zeolite pores or cages, and the basicity of the zeolite is easily varied by ion exchange with Group IA or IIA cations. The use of a zeolite support to restrict metal particle size may seem to be counterproductive since ammonia synthesis is well-recognized to be a structure sensitive reaction. However, ammonia synthesis on Ru catalysts is not as greatly affected by particle size as on Fe catalysts (6). In fact, single crystal studies found that N_2 dissociation was independent of the exposed Ru surface plane (7). Since N_2 adsorption is generally regarded as the rate determining step in ammonia synthesis, the reaction may actually be structure insensitive on Ru. The importance of these findings cannot be overstated. They suggest that, assuming suitable promoters are found, very small clusters of Ru can be as active as bulk Ru metal for ammonia synthesis. Extremely high dispersions of Ru metal are needed to minimize the cost associated with these new catalysts.

Ammonia synthesis catalyzed by ruthenium supported on alkali-metal-exchanged zeolites X and Y has been studied recently by Cisneros and Lunsford (8). Even though their materials were catalytically active at atmospheric pressure over the temperature range 573–723 K, the turnover frequencies were inferior to other promoted Ru catalysts. However, since the metal was highly dispersed, the Ru/zeolites were comparable in activity to other Ru catalysts when rates were based on the total number of ruthenium atoms in the sample. Cisneros and Lunsford also found that the activity of zeolite-supported ruthenium was strongly dependent on the cations present in the zeolite—the more basic the zeolite, the more active the catalyst. The general consensus regarding supported Ru catalysts is that promoter effectiveness increases with basicity.

We recently investigated the catalytic activity of a series of well-exchanged alkali and alkaline earth X zeolites,

0021-9517/98 $25.00

loaded with 2 wt% Ru (9, 10). The activities of these catalysts for ammonia synthesis were measured in a closed-loop recirculation reactor at atmospheric total pressure with a stoichiometric mixture of dinitrogen and dihydrogen. The turnover frequency on Ru/CsX was greater than that on Ru/KX, which was anticipated since the high level of cesium exchange rendered CsX more basic than KX. However, Ru clusters supported on alkaline earth zeolites were much more active than those on alkali-exchanged zeolites, exceeding the turnover frequencies on Ru/CsX by a factor of 3 or 4. This was totally unexpected given earlier work that showed Ba to be a less effective promoter than Cs for Ru/MgO (6), and Ba and Cs to be about equally effective as promoters for Ru/carbon (11). In addition, alkaline earth zeolites are less basic than alkali zeolites.

In this paper, we expand upon the new concepts introduced above. Specifically, the effects of cation type (alkali or alkaline earth) and loading (partial ion exchange or occluded extra-framework species) on the kinetics of ammonia synthesis at 20 bar over zeolite-supported Ru clusters are investigated.

EXPERIMENTAL METHODS

Catalyst Preparation

Consistent with our previous work (9, 10), the starting material for the zeolite catalysts was a potassium X zeolite obtained by a triple ion exchange of NaX (Union Carbide) with a 1M KNO_3 solution for 24 h at room temperature. A 2 wt% loading of Ru was accomplished by ion exchange of the KX zeolite with an aqueous solution of $Ru(NH_3)_6Cl_3$. After washing of the Ru^{3+} exchanged compounds with deionized distilled water, the absence of chloride was confirmed by silver nitrate tests of the filtrates. The Ru/KX samples were then reduced before any further modifications. A sample was first dehydrated by heating in dynamic vacuum at a rate of 0.5 K min^{-1} to 723 K (final pressure less than 10^{-4} mbar) and holding at that temperature for 1 h. The materials were cooled to room temperature in vacuum before being exposed to H_2 (palladium purified) flowing at 20 cm^3 min^{-1} g^{-1}. The temperature was then ramped by 1 K min^{-1} to 723 K and held for 2 h. Afterwards, the sample was cooled in vacuum (final pressure less than 10^{-5} mbar) and exposed to atmosphere.

The reduced Ru/KX material was used to prepare Ru/CsX, Ru/MgX, and Ru/BaX. The Ru/KX was ion-exchanged three times at room temperature in 1 *M* solutions of Cs, Mg, or Ba acetate, filtered, and washed. Acidic sites that were created during the reduction of ruthenium or subsequent catalyst modifications were partially or totally neutralized by incipient wetness impregnation of the samples with aqueous solutions of KOH, CsOH, $Mg(OH)_2$, or $Ba(OH)_2$ equal to or less than 0.2 molal in concentration. In some cases, the amounts of hydroxide added resulted in cationic loadings exceeding the ion exchange capacity of the zeolites.

A Ru/CsMgO compound was also prepared as a reference material. Ruthenium (2 wt%) was loaded onto magnesia (Ube Industries) by impregnation with $Ru_3(CO)_{12}$ dissolved in THF. This sample was then reduced according to the same procedure described above. Cesium was added as a promoter by impregnation with aqueous cesium acetate. The acetate was decomposed by heating the sample at 1 K min^{-1} to 773 K in flowing N_2 (50 cm^3 min^{-1} g^{-1}). It should be mentioned here that other MgO-supported catalysts were also prepared by using MgO derived from calcination of solid $Mg(OH)_2$ in flowing air at 773–873 K. Even though the supports had a high surface area, the resulting Ru catalysts were orders of magnitude less active than the sample prepared from Ube MgO. Magnesia purity and/or crystallinity are likely to be important factors in the preparation of Ru clusters for ammonia synthesis.

Elemental analyses of the catalysts were performed by Galbraith Laboratories (Knoxville, TN).

Gas Adsorption

Dinitrogen adsorption isotherms were obtained on samples dehydrated in vacuum at 573 K (final pressure less than 10^{-6} mbar), using a Coulter Omnisorp 100CX instrument. Specific surface areas and pore volumes were used to check the crystallinity of our samples. Micropore volume was determined from the uptake of dinitrogen at 77 K at a relative pressure of 0.3. The same apparatus was used to carry out H_2 chemisorption experiments. Before chemisorption, the samples were heated at 1 K min^{-1} in flowing dihydrogen to 663 K for 30 min and outgassed in high vacuum at 673 K for 45 min (final pressure was less than 10^{-6} mbar). The samples cooled down in vacuum to the adsorption temperature of 303 K. Dihydrogen (99.999%, BOC Gases) was purified through an OMI-2 purifier (Supelco, Inc.) before admission to the system. The total amount of dihydrogen chemisorbed was calculated by extrapolating the linear part of the adsorption isotherm to zero pressure. The amount of reversibly adsorbed dihydrogen was evaluated by evacuating the sample at 303 K and recording a backsorption isotherm. The amount of irreversibly adsorbed dihydrogen was calculated from the difference between the isotherms. The turnover frequencies reported in this work are based on surface metal sites counted by the number of hydrogen atoms adsorbed irreversibly on the clusters.

Catalytic Reaction

The ammonia synthesis reaction was carried out in a stainless steel fixed bed reactor system (model BTRS-Jr, Autoclave Engineers). Before entering the catalyst bed, the reactant gases (99.999% pure) passed through a guard bed

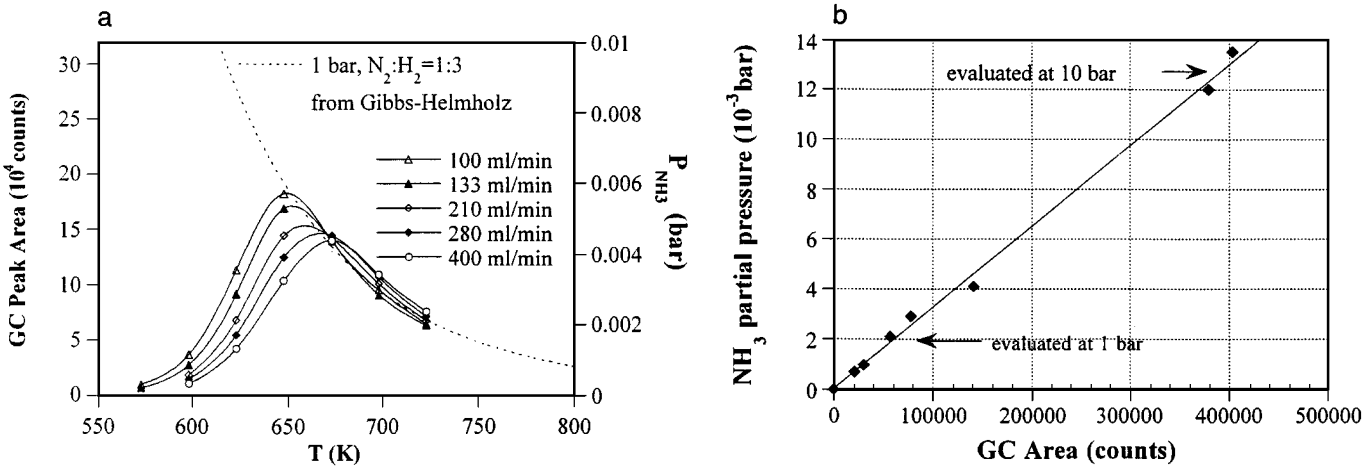

FIG. 1. (a) Plot of the temperature dependence of gas phase composition at thermodynamic equilibrium (catalyst: Ru/CsMgO, 1 bar, $N_2 : H_2 = 1 : 3$). The GC response for ammonia is shown for the different total flow rates versus temperature and can be directly compared to the ammonia partial pressure determined by thermodynamic calculations (deduced from the Gibbs–Helmholtz equation). (b) Linear response of the TCD with the ammonia partial pressure. Ammonia partial pressures are deduced from the thermodynamic calculations (see Fig. 1a) at 1 bar and from the experimental results of Larson *et al.* (12) at 10 bar.

consisting of MnO/SiO_2 and molecular sieves to remove traces of dioxygen and water. Typically, one gram of catalyst was sieved to −40/+60 mesh (between 425 and 250 μm) and used for catalytic measurements. The catalyst was pretreated *in situ* to 723 K (heating rate of 1 K min^{-1}) in a stoichiometric mixture of N_2 and H_2 flowing at 130 cm^3 min^{-1}. The effluent ammonia concentration was measured on a gas chromatograph equipped with a thermal conductivity detector. The system was calibrated for ammonia response at very low concentrations by using the peak areas obtained from experimental runs at 1 and 10 bar that were allowed to reach thermodynamic equilibrium. These areas were then compared with concentrations derived from either equilibrium calculations or reported experimental results (12); the thermodynamic equilibrium values were calculated using the enthalpy polynomial coefficients for dinitrogen, dihydrogen and ammonia from Christiansen and Kjær (13). Figures 1a and 1b show the results from these calibration experiments and confirm the linear response of the detector in the range of ammonia concentrations used here.

The kinetic parameters were evaluated from 598 to 723 K, using $P_{N_2} : P_{H_2}$ ratios from 1 : 3 to 3 : 1 and variable total flowrates. The reaction order with respect to NH_3 was determined with a stoichiometric feed composition by varying the synthesis gas flow between 100 and 400 cm^3 min^{-1}; the reaction orders with respect to N_2 and H_2 were obtained at a constant flow rate (400 cm^3 min^{-1}), using He as a diluent. In general, all rates were evaluated at conditions far from thermodynamic equilibrium. Thirty percent of equilibrium conversion was attained on the most active catalyst at the highest temperature studied. No catalyst deactivation was observed after 15 days on stream.

RESULTS

Elemental Analysis

The chemical compositions of the compounds, expressed in terms of an ideal zeolite unit cell having 384 oxygen atoms bridging Si and Al tetrahedra, are summarized in Table 1. Protons were added to the unit cell formulas in order to balance the framework charge. Such acidic sites could have been formed during the Ru reduction (virtually 3 H^+ per Ru atom) and the several exchange and wash steps. The protons were progressively neutralized by successive impregnations of the catalysts with hydroxide solutions. Additional loadings of alkali or alkaline earth above the total ion-exchange capacity of the catalysts deposited extra-framework cations; Ru/KX-3, Ru/BaX-3, and Ru/BaX-4 appeared to possess extra-framework promoters. All the catalysts had a similar

TABLE 1

Elemental Analyses of the Supported Ru Catalysts

Catalyst	Ru loading (wt%)	Support composition by unit cell
Ru/KX-1	2.16	$Ru_{3.8}$ $Na_{3.8}$ $K_{65.6}$ $H_{15.1}$ $Al_{84.5}$ $Si_{107.5}$
Ru/KX-2	2.35	$Ru_{3.8}$ $Na_{4.0}$ $K_{73.3}$ $H_{7.9}$ $Al_{85.2}$ $Si_{106.8}$
Ru/KX-3	1.67	$Ru_{3.3}$ $Na_{5.1}$ $K_{97.0}$ $Al_{88.4}$ $Si_{103.6}$
Ru/KX-4	2.13	$Ru_{3.6}$ $Na_{4.2}$ $K_{64.7}$ $Ba_{6.9}$ $H_{2.8}$ $Al_{85.5}$ $Si_{106.5}$
Ru/CsX	1.82	$Ru_{3.9}$ $Na_{2.8}$ $K_{22.3}$ $Cs_{42.1}$ $H_{17.6}$ $Al_{84.8}$ $Si_{107.2}$
Ru/MgX	2.21	$Ru_{3.6}$ $Na_{3.4}$ $K_{34.1}$ $Mg_{17.9}$ $H_{10.7}$ $Al_{84.5}$ $Si_{107.5}$
Ru/BaX-1	2.02	$Ru_{3.8}$ $Na_{2.1}$ $K_{9.6}$ $Ba_{31.4}$ $H_{9.6}$ $Al_{84.5}$ $Si_{107.5}$
Ru/BaX-2	1.98	$Ru_{3.6}$ $Na_{1.9}$ $K_{8.6}$ $Ba_{35.4}$ $H_{3.4}$ $Al_{84.7}$ $Si_{107.3}$
Ru/BaX-3	1.68	$Ru_{3.4}$ $Na_{1.7}$ $K_{8.4}$ $Ba_{43.1}$ $Al_{85.0}$ $Si_{107.0}$
Ru/BaX-4	1.36	$Ru_{3.4}$ $Na_{4.2}$ $K_{10.7}$ $Ba_{52.3}$ $Al_{87.6}$ $Si_{104.4}$
Ru/CsMgO	1.98	Cs loading 5.47 wt%; Cs/Ru = 2

TABLE 2

Results from H_2 Chemisorption and N_2 Physisorption

Catalyst	H/Ru_{total}	$H/Ru_{irrever.}$	Specific surface area ($m^2\ g^{-1}$)		
			Unloaded support[a]	Before reaction	After reaction
Ru/KX-1	0.83	0.51	535	493	436
Ru/KX-2	1.04	0.64	—	465	478
Ru/KX-3	1.46	1.06	—	388	230
Ru/KX-4	1.06	0.63	—	484	454
Ru/CsX	0.52	0.30	337	300	217
Ru/MgX	0.75	0.45	491	495	483
Ru/BaX-1	0.85	0.42	499	461	454
Ru/BaX-2	0.81	0.40	493	436	451
Ru/BaX-3	0.86	0.47	448	410	367
Ru/BaX-4	0.89	0.45	—	407	289
Ru/CsMgO	1.15	0.69	100	96	33

[a] Supports with the same exchange and impregnation procedures, but without ruthenium.

content of Ru (∼2 wt%), comprising between 3.4 and 3.9 metal atoms per unit cell.

Since ammonia synthesis on Ru may be affected by surface structure, samples having similar Ru cluster sizes are required to confidently attribute any differences in observed turnover frequencies to the presence of promoters. Since no Ru phases were detected by X-ray diffraction on any of the samples, the clusters sizes were in the nanometer size range. Table 2 lists the total and irreversible amount of chemisorbed hydrogen atoms per Ru atom. The amount of hydrogen chemisorbed on the ruthenium clusters did not vary to a large extent for our catalysts, indicating the zeolite support allows for the formation of fairly uniform clusters regardless of the compensating cation. Furthermore, the Ru clusters supported on Cs-promoted MgO had a comparable dispersion, enabling the sample to be used as a reference catalyst. Interestingly, addition of either potassium or barium to Ru/KX-1 increased the amount of adsorbed hydrogen, whereas addition of barium to Ru/BaX-1 did not enhance the hydrogen uptake. An explanation for the unusual observations on the Ru/KX samples is not known at this time.

The Ru/CsX material revealed an atypically low dihydrogen adsorption capacity, which might be explained by a partial loss of the zeolite framework crystallinity. Table 2 shows the specific surface areas of the different materials, both before and after the ammonia synthesis reaction. The relatively low specific surface area of Ru/CsX compared to Ru/KX-1 is consistent with a partial loss in crystallinity, even after accounting for the difference in cation atomic weights. This conclusion is also supported by the micropore volumes reported in Table 3. Since volumes are based on numbers of unit cells instead of total catalyst weight, the heavy atomic weight of Cs does not contribute to the low specific micropore volume. The Ru/CsX sample had the lowest initial micropore volume of all samples studied, indicating significant loss in crystallinity and/or displacement of free volume due to the large size of Cs cations.

The specific surface area and micropore volume of Ru/KX-3 was affected by both catalyst preparation and catalytic testing. The decrease in surface area and volume after preparation is easily explained by the high cation loading: in addition to all the exchange sites being occupied by K^+, each supercage contained, on average, 1.7 extra cations. The significant decrease in surface area and volume of Ru/KX-3 after the ammonia synthesis reaction was likely due to a partial loss of crystallinity. A Ru/BaX sample containing extra-framework Ba (Ru/BaX- 4) also lost surface area and micropore volume due to reaction, but to a lesser extent than Ru/KX-3. Apparently, the strong basicity of the extra-framework species located inside the pores destabilized the zeolite support under ammonia synthesis conditions. Since alkali oxides and hydroxides are stronger bases than corresponding alkaline earth compounds, the greater loss in surface area and micropore volume for Ru/KX-3 compared to Ru/BaX-4 is reasonable. All other zeolite-based catalysts presented high surface areas, even after ammonia synthesis.

Catalyst Reactivity

Each catalyst was tested in the ammonia synthesis reaction at different temperatures and reactant mixture compositions at 20 bar. Figure 2 is a typical plot of the ammonia synthesis rate as functions of N_2, H_2, or NH_3 partial pressures. Reaction orders, determined far from thermodynamic equilibrium, are summarized in Table 4. In all cases, a

TABLE 3

Micropore Volume of Supported Ru Catalysts

Catalyst	Micropore volume (cm^3 (mol unit cells)$^{-1}$)		$\Delta V/V^a$ (%)	H^+ per u.c.[b]
	Before reaction	After reaction		
Ru/KX-1	3477	3117	−10	15
Ru/KX-2	3376	3459	+3	8
Ru/KX-3	2985	1769	−41	(a)
Ru/KX-4	3645	3430	−6	3
Ru/CsX	2703	1951	−28	18
Ru/MgX	3323	3237	−3	11
Ru/BaX-1	3745	3694	−1	10
Ru/BaX-2	3644	3776	+4	3
Ru/BaX-3	3635	3241	−11	(b)
Ru/BaX-4	3889	2758	−29	(c)

[a] Percentage change in micropore volume due to reaction.

[b] Protons per unit cell (u.c.) determined from chemical analysis reported in Table 1.

(a) Extra-framework potassium species: K^+_{extra}/u.c. = 13.7.

(b) Extra-framework barium species: Ba^{2+}_{extra}/u.c. = 5.7.

(c) Extra-framework barium species: Ba^{2+}_{extra}/u.c. = 16.

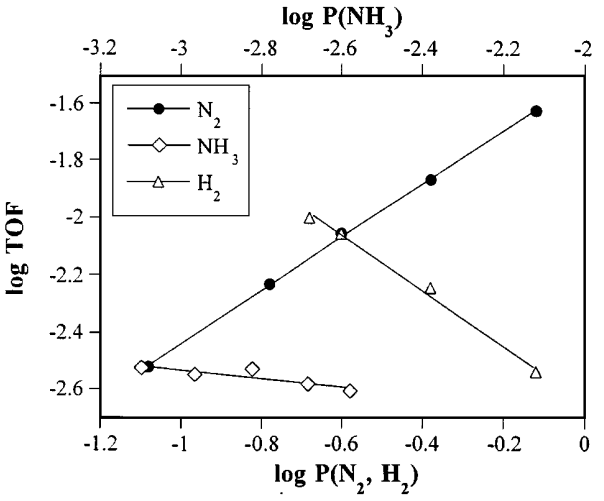

FIG. 2. Dependence of the ammonia synthesis rate on dinitrogen, dihydrogen, and ammonia partial pressures (20 bar, 623 K) over Ru/BaX-4. For determination of the orders in N_2 and H_2, the turnover frequencies at constant ammonia pressure have been considered.

nearly first-order dependence on dinitrogen was observed. Even though most of the catalysts revealed an order in dihydrogen of negative one, a few cases were even more inhibited by H_2. The Ru/KX-2 material was inhibited strongly by H_2 with a reaction order of -1.75. The synthesis reaction was slightly, but measurably, inhibited by ammonia on all of the catalysts.

According to the work of Holzman *et al.* (14) concerning the importance of the ammonia partial pressure on the reaction kinetics over supported ruthenium, we recalculated the turnover frequencies (673 K) and the activation energies at 20 bar at a constant ammonia pressure using the reaction orders determined experimentally. These values, given in Table 5 for a stoichiometric feed mixture, are compared with the measured ones obtained from constant flow experiments. The apparent activation energies at 20 bar range from 124 to 181 kJ mol^{-1}, if the anomalously low value for Ru/CsX is not included. We believe this is justified because the CsX support had a very low micropore volume and contained the most protons per unit cell of any sample.

TABLE 4

Orders of Reaction for Ammonia Synthesis over Supported Ru Catalysts at 20 bar[a]

Catalyst	Temperature (K)	α (N_2)	β (H_2)	γ (NH_3)
Ru/KX-1	698	1.01	−1.10	−0.16
Ru/KX-2	673	1.11	−1.75	−0.10
Ru/KX-3	673	1.13	−1.29	−0.15
Ru/KX-4	648	1.17	−1.68	−0.12
Ru/CsX	723	1.24	−1.03	−0.38
Ru/MgX	673	0.91	−0.75	−0.40
Ru/BaX-1	673	0.74	−0.92	−0.05
Ru/BaX-2	648	0.97	−1.27	−0.24
Ru/BaX-3	648	0.96	−0.96	−0.20
Ru/BaX-4	623	0.93	−0.96	−0.15
Ru/CsMgO	623	1.08	−1.14	−0.08

[a] According to the reaction rate equation $r = k\, P_{N_2}^{\alpha} P_{H_2}^{\beta} P_{NH_3}^{\gamma}$.

TABLE 5

Rates of Ammonia Synthesis over Supported Ru Catalysts at 20 bar and Stoichiometric Feed

Samples	TOF c.f.[a] (10^{-4} s^{-1})	E_a[b] (kJ mol^{-1})	TOF c.p.[c] (10^{-4} s^{-1})	E_a c.p.[d] (kJ mol^{-1})
Ru/KX-1	14.8	113	12.9	124
Ru/KX-2	22.7	121	22.3	132
Ru/KX-3	20.7	133	21.5	141
Ru/KX-4	37.7	146	39.1	163
Ru/CsX	21.9	94	15.3	82
Ru/MgX	39.1	105	35.6	147
Ru/BaX-1	28.5	166	27.5	173
Ru/BaX-2	68.6	146	76.7	181
Ru/BaX-3	137	126	178	157
Ru/BaX-4	197	125	252	151
Ru/CsMgO	405	128	497	143

[a] Turnover frequencies measured at constant flow rate (400 cm^3 min^{-1} g^{-1}) and 673 K.

[b] Activation energies calculated at constant flow rate.

[c] Turnover frequencies at 673 K calculated at constant ammonia partial pressure ($P_{NH_3} = 0.001$ bar at standard conditions) using the experimental orders in ammonia reported in Table 3: $r = k'\,[NH_3]^{\gamma}$ since $[N_2]$ and $[H_2]$ were constant (low conversion).

[d] Activation energies calculated from turnover frequencies at constant ammonia pressure.

Table 3 indicates that the number of protons per unit cell was about 10 for both Ru/MgX and Ru/BaX-1. Thus, a fair comparison of catalytic results should include Ru/KX-1 and Ru/KX-2, which contain 15 and 8 protons per unit cell, respectively. The turnover frequencies on Ru/MgX and Ru/BaX-1 at 673 K were greater than those on Ru/KX-1 or Ru/KX-2, indicating that alkaline earth zeolites are better supports than alkali zeolites for catalytically active Ru clusters.

Figure 3 compares the activities of the Ru/KX-1 catalyst with samples to which were added different loadings of potassium hydroxide (Ru/KX-2 and Ru/KX-3) or Ba hydroxide (Ru/KX-4). From Table 5, addition of about $M/\mathrm{Ru} = 2$ (M = K or Ba) leads to an increase in activity of about 70% for potassium (Ru/KX-2) and 200% for barium (Ru/KX-4). Even added in a small amount to a KX zeolite, barium promoted supported Ru. When additional potassium was added to a Ru/KX zeolite (Ru/KX-3), the activity did not continue to increase with loading. This observation was probably due to the fact that the higher loaded potassium material lost 48% of its micropore volume during the catalytic test. Since the catalyst did not show any deactivation during the runs, the loss in crystallinity likely occurred during the catalytic pretreatment or very early in the run. Interestingly, the activation energies increased with

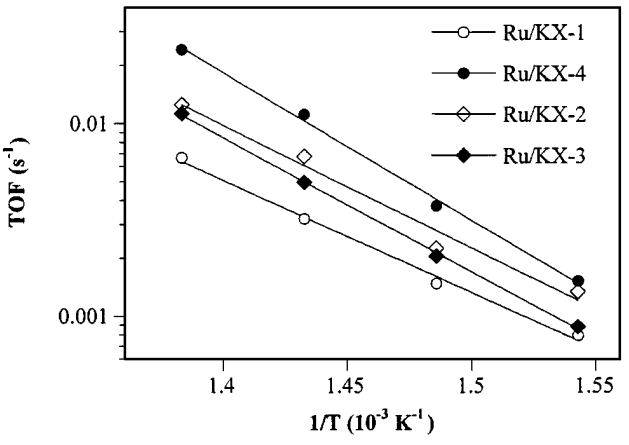

FIG. 3. Turnover frequencies for ammonia synthesis at 20 bar on Ru/KX zeolite neutralized with different amounts of potassium or barium ($N_2 : H_2 = 1 : 3$, 400 cm^3 min^{-1} g^{-1}).

potassium content. These results are similar to the trend reported by Muhler *et al.* (15) on Ru/MgO and Ru/Al_2O_3 in which the addition of cesium (Cs/Ru = 3) provoked an increase in E_a by more than 20 kJ mol^{-1}.

Because of the beneficial effect of alkaline earth ions, we investigated the catalytic activity of several samples containing various loadings of barium. Table 3 indicates that the number of protons per unit cell is lower in Ru/BaX-2 compared to Ru/BaX-1 due to hydroxide addition. Additional loading of barium in Ru/BaX-3 and Ru/BaX-4 resulted in the elimination of protons and the occlusion of extra-framework barium cations. For these latter two samples, the amount of extra-framework barium was Ba_{extra}/Ru = 1.7 and 4.7, respectively. The turnover frequencies measured over these catalysts and Ru/CsMgO are shown in Fig. 4. The activity of the zeolite catalysts increased monotonically with the loading of barium and approached the activity of

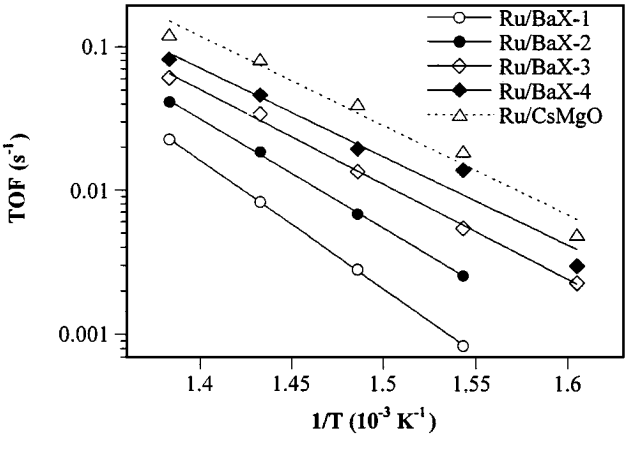

FIG. 4. Turnover frequencies for ammonia synthesis at 20 bar on Ru/BaX zeolite with different loadings of barium hydroxide ($N_2 : H_2 = 1 : 3$, 400 cm^3 min^{-1} g^{-1}).

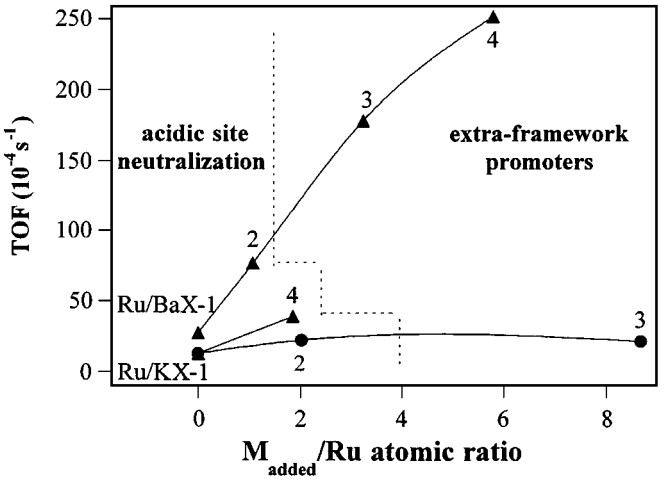

FIG. 5. Influence of promoter loading on ammonia synthesis turnover frequencies (20 bar, 673 K, $N_2 : H_2 = 1 : 3$) over zeolite-supported Ru catalysts. The dotted line indicates the estimated amount of added promoter needed to neutralize the catalysts.

Ru/CsMgO. The difference in activity between Ru/BaX-1 and Ru/BaX-4 was almost one order of magnitude.

Figure 5 summarizes the beneficial effect of Ba on the activity of zeolite-supported Ru. For comparison, the results from the potassium-loaded samples are also included. Barium exchange and impregnation both neutralize protonic sites (Ba^{2+} located at the exchange sites) and promote the ammonia synthesis reaction. Remarkably, the increase of the turnover frequency was proportional to the amount of barium added. Also, as seen in Fig. 4 and Table 5, addition of barium caused the apparent activation energies to decrease from 173 to 151 kJ mol^{-1}.

DISCUSSION

Results from this work at elevated pressure confirm earlier findings obtained at atmospheric pressure that Ru supported on zeolites are highly active catalysts for the ammonia synthesis reaction (9, 10). Furthermore, alkaline-earth-exchanged zeolites are more effective supports than alkali-exchanged Ru/X materials, which again is consistent with our previous work (9, 10). Since the dispersion of ruthenium was similar for each of our catalysts, cluster size effects can be dismissed as a major cause for the observed differences. Cisneros *et al.* reported that turnover frequencies for alkali-promoted Ru/X ammonia synthesis catalysts are correlated to the partial negative charge of the oxygen atoms in the zeolite framework (8). Partial charges were calculated from the Sanderson electronegativities of the elements comprising the zeolites. However, our results do not conform to the relationship proposed by Cisneros *et al.*; all Ru/BaX samples have less negative partial oxygen charges than Ru/KX samples, but the Ba-containing samples have greater activities.

Results in Table 3 provide some insight into the role of promoters. Catalyst samples having the highest estimated proton contents lost some micropore volume due to reaction. We assume this loss of crystallinity occurred during the catalytic pretreatment or very early in the run since deactivation was not observed over a period of 15 days. Previous studies on the thermal stability of faujasite zeolites showed that the ammonium form of zeolite X is fragile compared with the alkali- or alkaline-earth-exchanged ones (16). Once promoters (KOH or $Ba(OH)_2$) were impregnated to neutralize the remaining protons in the zeolite, the micropore volume was essentially unchanged by catalytic reaction. Thus, preparation of a fully exchanged zeolite may be necessary to obtain a stable material. Since twice the amount of potassium is needed theoretically to neutralize the same number of acid sites as barium, the lower activity of Ru/KX may also result from partial pore blockage. Table 3 shows that, in general, Ru/BaX has greater micropore volume per unit cell than analogous Ru/KX. This conclusion contrasts our earlier work with similar materials (9). Therefore, the role of pore blockage by cationic promoters is not completely clear at this time. However, we currently believe that the beneficial effect of Ba is not attributable to reduced steric constraints in the vicinity of the Ru cluster since earlier work with Ru supported on non-microporous silica also found significant promotion by Ba (9).

The protons formed in our compounds are probably generated during reduction of $Ru(NH_3)_6^{3+}$ and excessive washing of the catalysts. It is likely that the ruthenium particles are mostly located in supercages where the acid sites remain. Samant *et al*. demonstrated on Pt/Y systems that the presence of acid sites induces an increase in ionization potential of the platinum clusters (17). On Ru/NaY catalysts, formation of metal–proton adducts creates electron-deficient Ru particles (18). A decrease of the Ru ionization potential by removing the protons from the zeolite may reduce the activation energy for dissociative adsorption of N_2 by enhancing electron transfer from the metal to the anti-bonding orbitals of dinitrogen. Since N_2 adsorption is generally regarded as the rate determining step in ammonia synthesis over ruthenium (19–22), such a modification of the ruthenium electronic structure may explain the higher activity of the neutralized zeolites. The low level of activity for Ru/CsX can be partially accounted for by its high proton content. Moreover, this finding suggests that Ru/MgX can be significantly improved by neutralizing the residual protons in the sample.

Loading of promoters beyond ion-exchange capacity also affected the activity of the catalysts. Overloading of promoter led to destabilization of the zeolite and partial loss in crystallinity. When a large amount of extra potassium was incorporated into the catalyst (13.7 cations per unit cell), the loss in micropore volume due to reaction was quite severe (−41%) and the promotional effect of alkali was masked. A similar loading of extra barium (16 cations per unit cell) resulted in a less severe loss in micropore volume (−29%) and substantial promotion of ammonia synthesis activity. Thus, one beneficial effect of extra-framework alkaline earth ions compared to extra-framework alkali ions may be related to zeolite crystallinty in the vicinity of the Ru clusters. Apparently, the zeolite maintains better structural integrity in the presence of the alkaline earth ions.

The extra-framework barium promoters were probably occluded in the zeolite supercages along with the Ru metal clusters. According to the studies of Murata *et al*. (6, 23, 24), promotion of ruthenium supported on a metal oxide may require contact between the promoter and the ruthenium. In our case, the extra-framework barium species are likely in close contact with the ruthenium clusters in light of their significant effect on reactivity. However, further study is needed to clarify the role of barium promoters during ammonia synthesis.

The rate-determining step in ammonia synthesis over Ru catalysts is believed to be the dissociative adsorption of N_2 because the reaction is first order in dinitrogen and no H_2/D_2 isotopic effect is observed (9, 19). Furthermore, Urabe *et al*. (20) found that the adsorption sites on ruthenium were occupied mostly by hydrogen atoms. In an earlier paper, we suggested that the kinetics of ammonia synthesis can be described by a reaction mechanism composed of dinitrogen adsorption as the rate determining step and both adsorbed hydrogen and nitrogen atoms as most abundant reactive intermediates (9). With those assumptions, the following expression for the forward rate of ammonia synthesis on a uniform surface can be derived,

$$r = k_1'[\mathrm{L}][\mathrm{N_2}]\left\{1 + [\mathrm{H_2}]^{1/2}\mathrm{K_2}^{-1/2} + \mathrm{K_3}\mathrm{K_2}^{3/2}[\mathrm{NH_3}][\mathrm{H_2}]^{-3/2}\right\}^{-2}, \quad [1]$$

where k_1' is the N_2 adsorption rate constant, [L] is the number density of active sites, K_2 is the inverse of the equilibrium constant for H_2 adsorption, and K_3 is an equilibrium constant for the surface reaction of nitrogen and hydrogen atoms to form ammonia (9). The order in dinitrogen is unity, the order in ammonia is negative or zero, and the order in dihydrogen can be either positive or negative, depending on which term in the denominator dominates.

As seen in Table 4, our highly active Ru/BaX and Ru/CsMgO catalysts exhibit reaction orders of approximately one for N_2, zero for NH_3 and negative one for H_2. These results indicate the term $[H_2]^{1/2}K_2^{-1/2}$ is much greater than the others in the denominator of Eq. [1], and the expression can be reduced to

$$r = k_1'\mathrm{K_2}[\mathrm{L}][\mathrm{N_2}][\mathrm{H_2}]^{-1}. \quad [2]$$

From this simplified expression, it is easy to see that the activation energy for the reaction is composed of the

activation energy for dinitrogen adsorption plus the heat of adsorption of dihydrogen on Ru. Hinrichsen *et al*. used temperature programmed adsorption/desorption and isotopic exchange reaction to measure the activation energy of dinitrogen adsorption on a variety of supported Ru catalysts, including Ru/Al_2O_3, Ru/MgO, and Ru/CsMgO (25). Depending on the support and promoter, the activation energy for dinitrogen adsorption ranged from 61 kJ mol^{-1} to 33 kJ mol^{-1}, the lowest value for the highly active Ru/CsMgO ammonia synthesis catalyst. The heat of adsorption for dihydrogen on zeolite-supported Ru clusters can be estimated from a variety of sources. For example, Danielson *et al*. (26) and Tsai and Weinberg (27) found an adsorption energy of 92 kJ mol^{-1} on a single crystal Ru (0001) surface. Narayan *et al*. used microcalorimetry of H_2 adsorption on Ru black and Ru/SiO_2 to arrive at an initial ΔH_{ads} of about 90 kJ mol^{-1} (28). In contrast to the above results, others have reported ΔH_{ads} on Ru as high as 110–115 kJ mol^{-1} (29, 30). For the sake of this discussion, we will assume that the ΔH_{ads} of dihydrogen on zeolite supported Ru clusters is about 100 kJ mol^{-1}. The effect of promoters on ΔH_{ads} is unclear at present. Narayan *et al*. found no effect of adding K to Ru on the initial ΔH_{ads} (28), whereas Fastrup reports that Cs significantly lowers ΔH_{ads} (30). Since the variation in ΔH_{ads} on transition metals across the periodic table from Mo to Pd is only about 50 kJ mol^{-1} (29), we will assume ΔH_{ads} is not affected greatly by promoters. The range of overall activation energies for ammonia synthesis based on Eq. [2], calculated from E_a (N_2 adsorption) plus ΔH_{ads} (H_2 adsorption), is about 161 to 133 kJ mol^{-1}. The lowest activation energy would correspond to the most active catalyst. The observed activation energies, calculated at constant ammonia pressure, for highly active Ru/BaX and Ru/CsMgO (Table 5) are consistent with the simplified mechanistic picture presented above.

Some of our samples have a reaction order in dihydrogen that is significantly less than −1, which cannot be explained by the kinetics represented in Eqs. [1] and [2]. In a recent paper, Fastrup explains how the ratio of adsorbed hydrogen atoms to adsorbed nitrogen atoms can lead to a reaction order in dihydrogen less than −1 for ammonia synthesis on Ru (30). For example, if the saturation coverage of hydrogen atoms is twice that of nitrogen atoms, Fastrup shows that the order of reaction in dihydrogen may actually range from −1.5 to −1.28. Clearly, refinements to our simple model are needed to explain the totality of our results; however, the reaction kinetics for our highly active Ru/BaX catalysts appear to be adequately described by the current model.

CONCLUSIONS

An opportunity for improvement in ammonia synthesis rates exists for zeolite-supported ruthenium catalysts if highly exchanged alkaline earth materials can be prepared, suggesting the importance of promoter proximity with the ruthenium particles. Moreover, addition of barium beyond ion exchange capacity can substantially enhance catalytic activity. It was confirmed in this study that alkaline earth cations are more effective promoters than alkali cations when loaded into zeolite catalysts, which is contrary to the ranking of zeolite basicity. In some cases, the strong basicity of added promoters can lead to local destruction of the zeolite framework.

Ammonia synthesis at 20 bar was generally first order in N_2 and minimally inhibited by product. The reaction order with respect to H_2 was always negative over our ruthenium catalysts, indicating that dihydrogen competes with dinitrogen for adsorption sites at elevated pressures. Interestingly, some of our least active catalysts were the most inhibited by dihydrogen. Therefore, in addition to enhancing the adsorption rate of dinitrogen, another possible role of alkaline earth promoters is to reduce the negative impact of dihydrogen on the ammonia synthesis rate. Additional studies are currently underway to clarify this point.

ACKNOWLEDGMENTS

This work was supported by the Academic Enhancement Program of the University of Virginia and the Dow Chemical Company. R.J.D acknowledges partial support provided by a U.S. National Science Foundation Young Investigator Award CTS-9257306.

REFERENCES

1. Ozaki, A., Aika, K.-I., Furata, A., and Okagami, A., U.S. Patent 3,770,658 (1973).
2. Aika, K.-I., Hori, H., and Ozaki, A., *J. Catal.* **27**, 424 (1972).
3. Chementator, A catalyst breakthrough in ammonia synthesis, *in* "Chemical Engineering," p. 19. 1993.
4. Goethel, P. J., and Yang, R. T., *J. Catal.* **111**, 220 (1988).
5. Baker, R. T. K., *Carbon* **24**, 715 (1986).
6. Aika, K.-I., Takano, T., and Murata, S., *J. Catal.* **136**, 126 (1992).
7. Dietrich, H., Geng, P., Jacobi, K., and Ertl, G., *J. Chem. Phys.* **104**, 375 (1996).
8. Cisneros, M. D., and Lunsford, J. H., *J. Catal.* **141**, 191 (1993).
9. Fishel, C. T., Davis, R. J., and Garces, J. M., *J. Catal.* **163**, 148 (1996).
10. Fishel, C. T., Davis, R. J., and Garces, J. M., *Chem. Commun.*, 649 (1996).
11. Aika, K.-I., Kawahara, T., Murata, S., and Onishi, T., *Bull. Chem. Soc. Jpn.* **63**, 1221 (1990).
12. Larson, A. T., and Dodge, R. L., *J. Am. Chem. Soc.* **45**, 2918 (1923).
13. Christiansen, L. J., and Kjær, J., "Enthalpy Tables of Ideal Gases," p. 1. Haldor Topsoe A/S, Copenhagen, 1982.
14. Holzman, P. R., Shiflett, W. K., and Dumesic, J. A., *J. Catal.* **62**, 167 (1980).
15. Muhler, M., Rosowski, F., Hinrichsen, O., Hornung, A., and Ertl, G., *Stud. Surf. Sci. Catal.* **101**, 317 (1996).
16. Breck, D. W., "Zeolite Molecular Sieves," p. 495. Krieger, Malabar, FL, 1984.
17. Samant, M. G., and Boudart, M., *J. Phys. Chem.* **95**, 4070 (1991).
18. McCarthy, T. J., Marques, C. M. P., Trevino, H., and Sachtler, W. M. H., *Catal. Lett.* **43**, 11 (1997).
19. Aika, K., and Ozaki, A., *J. Catal.* **16**, 97 (1970).

20. Urabe, K., Aika, K.-I., and Ozaki, A., *J. Catal.* **42**, 197 (1976).
21. Rambeau, G., and Amariglio, H., *J. Catal.* **72**, 1 (1981).
22. Aika, K., Kumasaka, M., Oma, T., Kato, O., Matsuda, H., Watanabe, N., Yamazaki, K., Ozaki, A., and Onishi, T., *Appl. Catal.* **28**, 57 (1986).
23. Murata, S., and Aika, K.-I., *J. Catal.* **136**, 110 (1992).
24. Murata, S., and Aika, K.-I., *J. Catal.* **136**, 118 (1992).
25. Hinrichsen, O., Rosowski, F., Hornung, A., Muhler, M., and Ertl, G., *J. Catal.* **165**, 33 (1997).
26. Danielson, L. R., Dresser, M. J., Donaldson, E. E., and Dickinson, J. T., *Surf. Sci.* **71**, 599 (1978).
27. Tsai, W., and Weinberg, W. H., *J. Phys. Chem*. **91**, 5302 (1987).
28. Narayan, R. L., Savargaonkar, N., Pruski, M., and King, T. S., *Stud. Surf. Sci. Catal.* **101**, 921 (1996).
29. Toyoshima, I., and Somorjai, G. A., *Catal. Rev.-Sci. Eng.* **19**, 105 (1979).
30. Fastrup, B., *Catal. Lett.* **48**, 111 (1997).